J Bone Miner Metab (2007) 25:36–45
DOI 10.1007/s00774-006-0725-9

ORIGINAL ARTICLE

**Mette Grøndahl Sørensen · Kim Henriksen
Sophie Schaller · Dennis Bang Henriksen
Finn Cilius Nielsen · Morten Hanefeld Dziegiel
Morten Asser Karsdal**

Characterization of osteoclasts derived from CD14+ monocytes isolated from peripheral blood

Received: April 6, 2006 / Accepted: August 30, 2006

Abstract Bone resorption is solely mediated by osteoclasts. Therefore, a pure osteoclast population is of high interest for the investigation of biological aspects of the osteoclasts, such as the direct effect of growth factors and hormones, as well as for testing and characterizing inhibitors of bone resorption. We have established a pure, stable, and reproducible system for purification of human osteoclasts from peripheral blood. We isolated CD14-positive (CD14+) monocytes using anti-CD14-coated beads. After isolation, the monocytes are differentiated into mature osteoclasts by stimulation with macrophage colony-stimulating factor (M-CSF) and receptor activator of nuclear factor κB ligand (RANKL). Osteoclast formation was only observed in the CD14+ population, not in the CD14– population, and only in the presence of both M-CSF and RANKL, confirming that the CD14+ system is a pure population of osteoclast precursors. No expression of osteoclast markers was observed in the absence of RANKL, whereas RANKL dose-dependently induced the expression of cathepsin K, tartrate-resistant acid phosphatase (TRACP), and matrix metallo proteinase (MMP)-9. Furthermore, morphological characterization of the cells demonstrated that actin rings were only formed in the presence of RANKL. Moreover, the osteoclasts were capable of forming acidic resorption lacunae, and inhibitors of lysosomal acidification attenuated this process. Finally, we measured the response to known bone resorption inhibitors, and found that the osteoclasts were sensitive to these and thereby provided a robust and valid method for interpretation of the effect of antiresorptive compounds. In conclusion, we have established a robust assay for developing osteoclasts that can be used to study several biological aspects of the osteoclasts and which in combination with the resorption marker CTX-I provides a useful tool for evaluating osteoclast function in vitro.

Key words human osteoclasts · CDM · morphology · resorption · osteoclastogenesis

M.G. Sørensen · K. Henriksen · S. Schaller · M.A. Karsdal (✉)
Nordic Bioscience A/S, Herlev Hovedgade 207, DK-2730 Herlev, Denmark
Tel. +45-44-52-5210; Fax +45-44-52-5251
e-mail: mk@nordicbioscience.com

D.B. Henriksen
Sanos Bioscience A/S, Rødovre, Denmark

F.C. Nielsen
Department of Clinical Biochemistry, University Hospital of Copenhagen, Denmark

M.H. Dziegiel
HS Blodbank, University Hospital of Copenhagen, Denmark

Introduction

The skeleton is a dynamic tissue that undergoes continuous remodeling throughout the life to sustain calcium homeostasis, repair microfractures, and react to strain and stress on the skeleton [1,2]. The continuous remodeling is dependent on the coupling between osteoclasts, the cells responsible for bone resorption, and osteoblasts, which are the cells responsible for bone formation [2,3]. Osteoclasts are large multinucleated cells arising through fusion of mononuclear hematopoietic stem cells found in the bone marrow, spleen, and peripheral blood [4–8]. The cytokines macrophage colony-stimulating factor (M-CSF) and receptor activator of nuclear factor κB ligand (RANKL) have been shown to be essential and sufficient for differentiation and activation of the osteoclasts [9]. The differentiation of osteoclasts is a complex multistep process involving commitment of cells from the monocyte lineage to differentiate into osteoclast precursors. The osteoclast precursors then undergo fusion to become mature multinuclear osteoclasts, which finally are activated to become bone-resorbing osteoclasts (Fig. 1) [1,10,11].

Resorbing osteoclasts are highly polarized cells containing different plasma membrane domains. A characteristic feature of resorbing osteoclasts is the formation of the sealing zone against the bone surface, which is a ring of filamentous actin fibers that in collaboration with the $\alpha_v\beta_3$ integrin

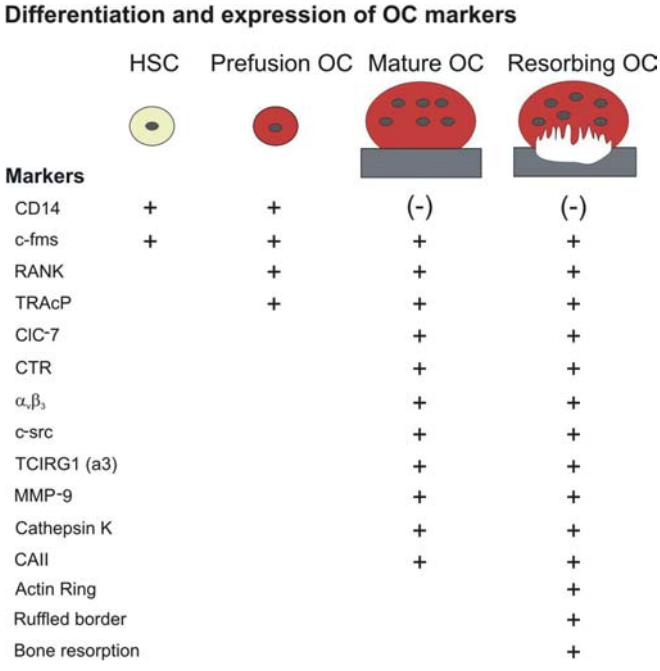

Fig. 1. Schematic illustration of the differentiation and activation of osteoclasts also illustrates the expression of osteoclast (*OC*) markers and the formation of the resorption lacunae

and the c-*src* tyrosine kinase seals of the resorption lacuna from the surroundings [12–14]. Inside the sealing zone the ruffled border membrane, which is a highly convoluted membrane, forms the actual "resorbing organ" [15]. Osteoclast mediated resorption of the mineralized bone matrix occurs via active secretion of protons through a V-ATPase [16–19], which is followed by passive transport of chloride ions, thereby maintaining electroneutrality [20,21]. The osteoclast V-ATPase contains an osteoclast-specific subunit, the a_3 subunit [22,23]. Loss of function mutations in the a_3 subunit leads to severe osteopetrosis in both humans and mice as a result of reduced acidification of the resorption lacunae [18,24]. Furthermore, the chloride channel required for acidification was shown to be ClC-7, and accordingly mutations lead to osteopetrosis [25]. The acidic environment in the resorption lacunae dissolves the hydroxyapatite matrix of the bone [26], while secretion of proteases, mainly cathepsin K, mediates degradation of the organic type I collagen matrix [27–31]. Loss of cathepsin K leads to pycnodysostosis, an osteopetrosis-like disease, characterized by accumulation of type I collagen fibers in the resorption pits [32,33]. Cathepsin K activity during resorption leads to generation of the resorption markers C-terminal cross-linked teleopeptide of type I collagen (CTX-I) and N-terminal crosslinked telopeptide of type 1 collagen (NTX) [34], which are valuable tools for studying osteoclast activities. Other hallmarks of osteoclasts are the expression of tartrate-resistant acid phosphatase (TRACP), the calcitonin receptor, $\alpha_v\beta_3$, and matrix metalloproteinase (MMP)-9, which all are known to play roles in osteoclast biology and therefore serve as useful tools for identification of osteoclasts [5,35–40].

Recently, it was found that osteoclasts precursors derive from CD14+ monocytes [41,42], and that M-CSF and RANKL are sufficient to drive osteoclastogenesis in vitro [9]. Thus, this study was aimed toward a further detailed characterization of the CD14+ human monocyte to osteoclast culture system. We isolated the CD14+ monocytes and cultured them in the presence of M-CSF and RANKL to induce osteoclastogenesis. We characterized their differentiation, expression of markers, morphology, resorption, and response to inhibitors of resorption, such as bafilomycin A1, NS5818, ethoxyzolamide, E64, GM6001, calcitonin, and pamidronate.

Materials and methods

Differentiation of osteoclast from CD14+ monocytes isolated from peripheral blood

The blood was received from the Danish University Hospital in Copenhagen as thrombocyte concentrates (buffy coats). The blood was first diluted 1:1 with phosphate-buffered saline (PBS) (BE17-512F Biowhittaker, Walkersville, MD, USA), and carefully layered on a Ficoll–Paque gradient (17-1440-03; Amersham Pharmacia, Burkinghamshire, UK). This gradient was centrifuged at 2000 rpm for 20 min. After centrifugation, the lymphocytes were collected from the interface between the plasma and the Ficoll–Paque. The cells were washed with ice-cold PBS, followed by centrifugation at 2000 rpm for 12 min. The wash was repeated twice, after which the cells were resuspended in cold PBS containing 2% serum (S0415 Biochrom, Cambridge, UK).

The cells were kept on ice while the beads were prepared. For 300 million cells, 125 µl anti-CD14-coated beads (10 million beads) were used. The tube with beads and ice-cold PBS was placed in the magnetic device for 2 min, after which the supernatant was discarded. This washing was repeated three times. Then, 300 million cells were added to the beads and incubated at 4°C with end-over-end homogenization for 20 min. After incubation at 4°C, the tube was placed in the magnetic device for 2 min, after which the supernatant was discarded. Hereafter, 5 ml PBS containing 2% serum was added, the beads were gently resuspended, and the tube was placed in the magnetic device for 2 minutes. This wash was repeated five times with gentle resuspension between each washing step. Finally, the cells were re-suspended in α-minimal essential medium (α-MEM) containing 10% fetal bovine serum, 100 units/ml penicillin, and 100 µg/ml streptomycin. The cells were seeded in 75 cm^2 bottles at a density of 150 000 cells/cm^2, and cultured for 3 days in α-MEM containing 10% serum, 100 units/ml penicillin, 100 µg/ml streptomycin, and 25 ng/ml M-CSF (216-MC R&D Systems, Minniapolis, MN, USA). The cells were incubated at 37°C in a humidified atmosphere with 5% CO_2. After culturing on tissue culture-coated plastic for 3 days, the monocytes were washed twice with PBS. Hereafter, trypsin was added and the cells were incubated

at 37°C for approximately 20 min. The cells were scraped off and reseeded on bovine cortical bone slices (cat. 1BON1000; Nordic Bioscience Diagnostics, Herlev, Denmark) at a density of 100 000 cells/well in a 96-well plate in α-MEM containing 10% serum, 100 units/ml penicillin, 100 μg/ml streptomycin, and 25 ng/ml M-CSF. The experiments were performed either with or without 25 ng/ml RANKL in the medium. The medium was changed every second day.

Isolation and culture of CD14– cells

The CD14– cells were isolated using the same procedure as the CD14+ cells (see above), with the modification that the cells not attached to the anti-CD14 beads were washed, seeded, and then cultured either in the presence of M-CSF (25 ng/ml) or the combination of RANKL and M-CSF (both at 25 ng/ml).

Mature osteoclasts for acidification, resorption, and array experiments

The osteoclasts were generated as previously described, with the modification that the full differentiation process was performed in tissue culture flasks. When a high level of osteoclasts with 3–5 nuclei was observed, the cells were lifted with trypsin and subsequent scraping with a rubber policeman. The lifted osteoclasts were then reseeded at a density of 50 000 cells per 96 wells on cortical bone slices and cultured for the desired time in medium containing M-CSF and RANKL and in the presence or absence of the various inhibitors described in the figure legends.

Cortical bovine bone slices

The bone slices were cut from sticks (cat. 1BON1000; Nordic Bioscience Diagnostics, Herlev, Denmark) that were made of cortical bone from cows. The sticks were cut into small slices 0.2 mm thick with a diameter that fits into 96-well plates.

Affymetrix array analysis

RNA from mature osteoclasts was isolated using trizol extraction. Two micrograms of purified RNA from the cultured osteoclasts was biotinlabeled and hybridized to the Affymetrix GeneChip Human Genome U133 Plus 2.0 Array, which contains approximately 54 000 probe sets according to the manufacturer's instructions. Three independent experiments were performed, and the individual samples were normalized using the invariant sets normalization method. The expression index computation and outlier detection were performed using the perfect-match-only model implemented in the dChip software package [43]. The results are shown as averages of the probe sets, compared to the average signal intensity on the array.

Osteoclast acidification assay

Acridine orange (3,6-bis[dimethylamine]acridine) at 10 μg/ml was loaded for 45 min in the culture medium in the presence or absence of various inhibitors. The dye was washed, and photographs were taken using an Olympus IX-70 microscope and an Olympus U-MWB filter (20× objective).

TRACP staining

The osteoclasts were fixed in 3.7% formaldehyde in PBS at the end of the culture period and TRACP stained using the Leukocyte Acid Phosphatase kit (cat. 387-A; Sigma-Aldrich, Copenhagen, Denmark). Digital micrographs were taken using a 20× objective and an Olympus C5050 Zoom digital camera mounted on an Olympus BX-60 microscope equipped with a 20× objective, and mounted in ImagePro (Media Cypernetics, Silverspring, MD, USA).

Immunocytochemistry

Immunocytochemistry was performed on osteoclasts seeded on bone slices. The osteoclasts were fixated in 3.7% formaldehyde in PBS and washed thoroughly in PBS. Thereafter, the cells were blocked for nonspecific binding and permeabilized in Tris-buffered-saline (TBS) containing 2.5% casein and 0.1% Triton X-100 (TBS-CT) for 30 min. This step was followed by incubation with the primary antibodies against cathepsin K (Chemicon International, Temecula, CA, USA), MMP-9 (kindly provided by L. Lund, The Finsen Laboratory, Copenhagen, Denmark) [44], ClC-7 (kindly provided by H. Solberg, Nordic Bioscience Diagnostics A/S, Herlev, Denmark) [45,46], TRACP, calcitonin receptor, and c-*src* diluted in TBS-CT overnight at 4°C, and then washing three times in TBS. As controls either the preimmune serum or the corresponding control IgG was used (data not shown). Furthermore, the cathepsin K, MMP-9, and ClC-7 antibodies were used for immunohistochemistry on human bone sections and all showed specific osteoclast localization in bone, confirming their specificity (data not shown). As a secondary antibody, either Rabbit or Mouse EnVision (Dakocytomation, Glostrup, Denmark) was used. The results were visualized using diamino benzidine (DAB)+ to generate a brown precipitate, and finally the bone slices were counterstained in Ehrlich's hematoxylin (BDH Laboratory Supplies, Poole, England) for 20 min, dehydrated and mounted in DPX.

For visualization of the actin cytoskeleton, Tetramethyl Rhodamine Iso-Thio-Cyanate (TRITC)-conjugated phalloidin (Sigma-Aldrich, Copenhagen, Denmark) was used. The procedure was performed as described above with omission of all the secondary steps.

All digital histographs were taken using an Olympus C5050 Zoom digital camera mounted on an Olympus BX-60 microscope equipped with a 20× objective, and for TRITC-phalloidin a U-MNG filter, and mounted in ImagePro (Media Cypernetics, Silverspring, MD, USA).

Western blotting

The CD14+ monocytes were seeded in 6-well plates and cultured in the presence of M-CSF and increasing concentrations of RANKL for 3, 6, 8, or 10 days, and then washed twice in ice-cold PBS before lysis in RIPA+++ buffer [47]. The lysates were then centrifuged 30 min at 15 000 *g* and 4°C to remove nonlysed fragments. The amount of protein was determined using the BioRad protein determination system (cat. 500-0111); 10 µg protein from each sample was diluted in sample buffer containing 80 mM dithiothreitol (DTT) and then run on a 10% sodium dodecyl sulfate-polyacry lamide gel electrophoresis (SDS-PAGE) gel, and subsequently transferred onto a nitrocellulose membrane. The nitrocellulose membranes were then blocked for nonspecific binding by incubation for 1 h at room temperature in TBS-T containing 5% skim milk powder. This step was followed by incubation with the primary antibody diluted in TBS-T milk over night. Then the membranes were washed in TBS-T three times, followed by incubation in the secondary peroxidase conjugated antibody. Finally, the membranes were washed in TBS-T three times, and the results were then visualized using the ECL system from Amersham Pharmacia (cat. RPN2109).

Measurement of TRACP activity

TRACP activity was measured by adding a colorimetric substrate in the presence of disodium tartrate to the conditioned medium after culturing the osteoclasts for a specific time period. The mixture was incubated for 1 h and the reaction was stopped with 0.3 M sodium hydroxide. The reaction products were quantified by measuring optical density at 405 nm.

Resorption pits

The resorption pits were visualized by washing the bone slices in milliQ water. The cell remains were removed by using a cotton swab. The pits were stained for 7–8 min in Mayer's hematoxylin, and finally the bone slices were washed in milliQ water. Digital micrographs were taken using a 20× objective and an Olympus C5050 Zoom digital camera mounted on an Olympus BX-60 microscope equipped with a 20× objective, and mounted in ImagePro (Media Cypernetics).

Resorption assays

The release of the c-terminal type I collagen fragments (CTX-I) from mineralized bone slices was determined using the CrossLaps for Culture kit (cat. 6CRL4000; Nordic Bioscience Diagnostics, Herlev, Denmark), according to the manufacturer's instructions.

Statistics

Statistical analyses were performed using an unpaired Student's *t* test, assuming normal distribution with equal variance. Statistical significance is shown by the number of asterisks: $P < 0.01$ = ** and $P < 0.001$ = ***.

Results

Osteoclast differentiation

To characterize osteoclast differentiation, we isolated a pure population of CD14+ monocytes using a CD14 antibody linked to an iron bead as described in the Materials and methods section. CD14+ cells were seeded at a cell density of 250 000/cm^2 on cortical bone slices and cultured in the presence of M-CSF alone or in combination with RANKL.

We measured TRACP activity and CTX-I release in the culture supernatants on all individual days of the experiment. As seen in Fig. 2A, both the CTX-I release and the TRACP activity were induced specifically in the presence of RANKL, showing that RANKL induces osteoclast differentiation and activity. Furthermore, we stained the osteoclasts for TRACP and the resorption pits using hematoxylin. Osteoclasts and resorption pits were only observed in the presence of RANKL (Fig. 2B).

Comparison of the osteoclastogenic potential of CD14+ and CD14– cells

To investigate whether only CD14+ cells were able to differentiate into osteoclasts, we compared the effect of either M-CSF alone or the combination of RANKL and M-CSF on CD14+ cells to the effect on CD14– cells.

We tested three concentrations of CD14– cells (100 000/cm^2, 250 000/cm^2, and 500 000/cm^2) and used the CD14+ cells as a positive control. We found that most of the CD14-negative cells were nonadherent and therefore were lost during the culture (data not shown). We investigated CTX-I release and TRACP activity in the conditioned medium of CD14– cells grown on bone. We found that the CD14– cells did not secrete TRACP and did not resorb bone at any time points (data not shown; also see Fig. 3A,B), whereas the CD14+ cells both secreted TRACP and resorbed bone, as expected [48]. In addition we performed TRACP staining on CD14– and CD14+ cells cultured for 16 days, and only the CD14+ cells cultured in the presence of both M-CSF and RANKL developed into mature multinuclear TRACP positive osteoclasts (Fig. 3C). In agreement with a previous publication, we obtained approximately 95% mature osteoclasts [48].

Affymetrix array analysis of osteoclasts

To investigate whether the osteoclast system expressed traditional osteoclast markers, we investigated mRNA

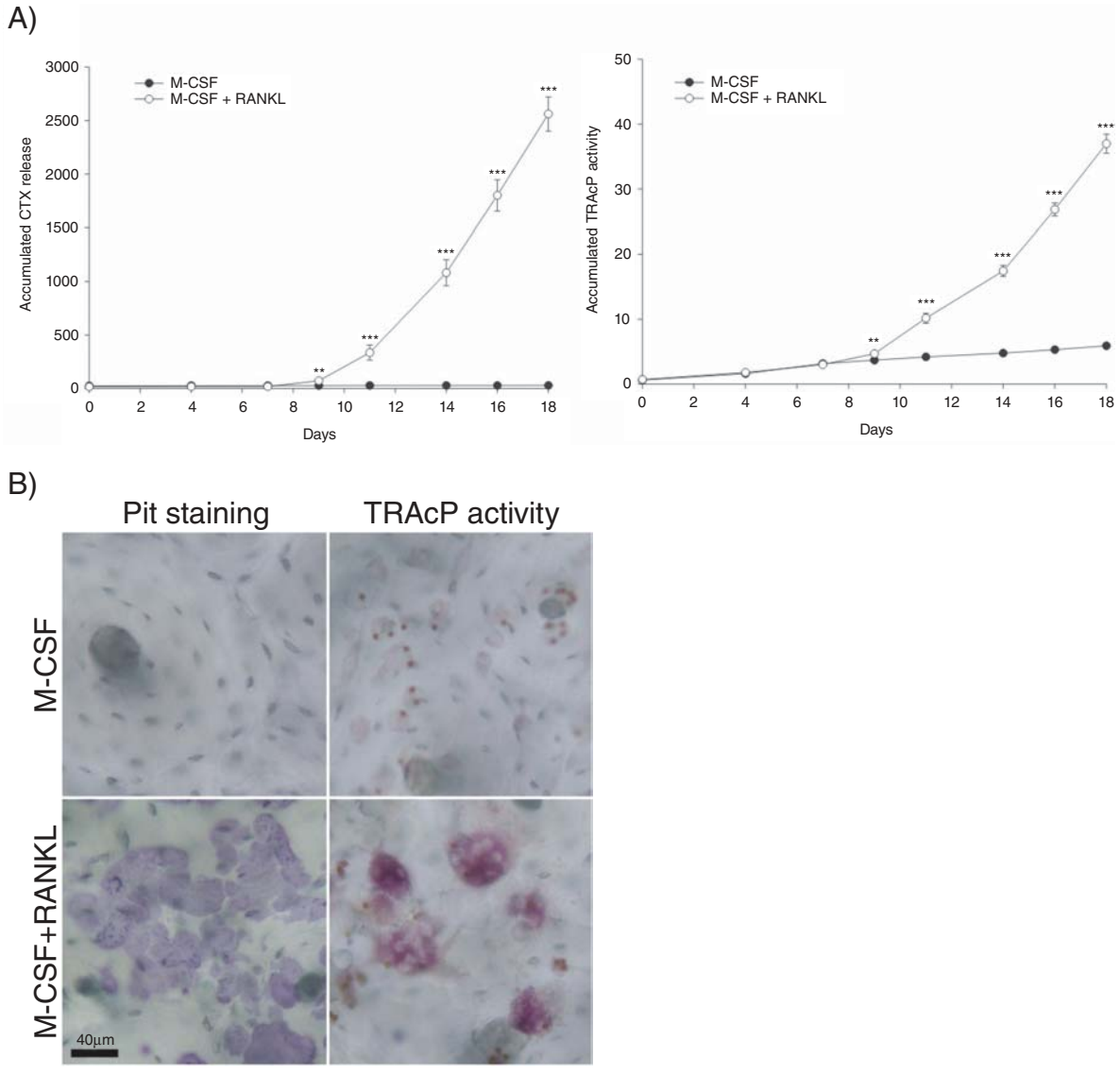

Fig. 2. Osteoclasts are only observed in the presence of RANKL. CD14+ monocytes were isolated as described in the Materials and methods section and cultured with macrophage colony-stimulating factor (M-CSF) alone or in combination with receptor activator of nuclear factor κB ligand (RANKL). The cells were grown for 18 days, and the C-terminal cross-linked teleopeptide of type I collagen (CTX-I) release and tartrate-resistant acid phosphatase (TRACP) activity were measured for all the days indicated in the figure (**A**). At the endpoint of the culture, the cells were stained for TRACP and the resorption pits were visualized using hematoxylin (**B**)

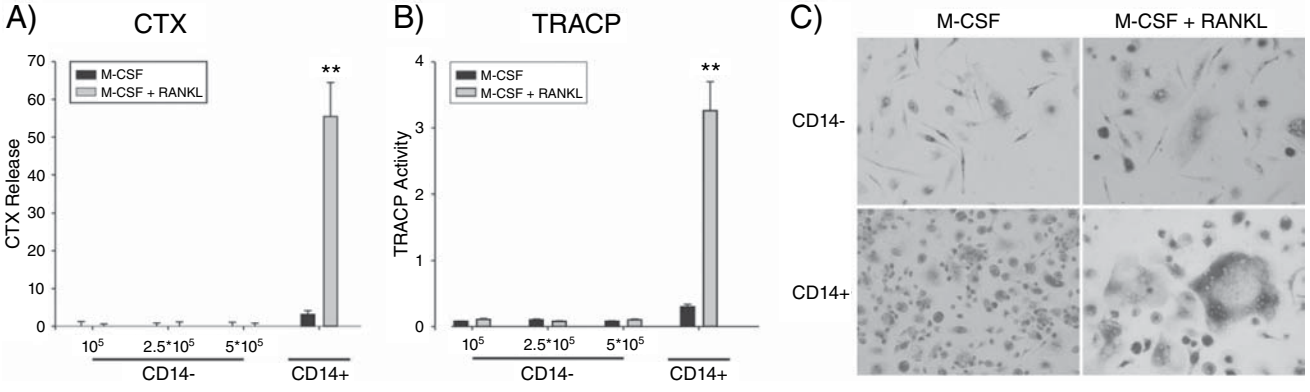

Fig. 3. CD14+ cells, but not CD14– cells, develop into mature osteoclasts. CD14+ or CD14– cells were isolated and seeded on either plastic or bone slices and cultured in the presence of M-CSF alone or the combination of RANKL and M-CSF. The cells were grown for 16 days and then CTX-I release and TRACP activity were quantified. TRACP staining was performed on the cells cultured on plastic. **A** CTX-I release in the supernatant at day 16 of the culture. **B** TRACP activity in the supernatant at day 16 of the culture. **C** TRACP staining of the cells at day 16 (20× magnification). *Asterisks* (**A,B**) indicate significant differences between M-CSF-treated CD14+ cells and M-CSF- + RANKL-treated CD14+ cells

expression of osteoclast markers using an affymetrix array. We cultured the osteoclasts on bone slices and isolated the mRNA using trizol extraction. The mRNA was hybridized to the affymetrix array, and the osteoclast marker expression was examined. Expression at least three times above the array average was observed for MMP-9, cathepsin K, TRACP, carbonic anhydrase II (CaII), α_v, c-*fms*, TCIRG1 (a_3), ClC-7, β_3, MT1-MMP, and c-*src*, showing that the cell population expresses several osteoclast markers at the mRNA level (Fig. 4).

Protein analysis of differentiating osteoclasts

To further characterize the osteoclastogenesis with respect to protein markers, we used Western blotting to analyze the expression of cathepsin K, MMP-9, and TRACP in cell lysates treated with different concentrations of RANKL at different days of culture. We used the p38 microtubule-associated protein kinase (MAPK) as a reference [48].

Figure 5 shows that at day 3 only TRACP is expressed at a low level, whereas neither cathepsin K nor MMP-9 is expressed. At day 8, a dose-dependent increase in expression of all the markers was seen; at day 10 all the RANKL conditions show equal expression of the osteoclast markers, whereas the M-CSF condition alone shows only low expression of TRACP, but no expression of cathepsin K and MMP-9. Expression of the p38 MAPK was seen in all conditions at all days.

Characterization of osteoclast morphology and marker localization

We investigated the morphology of CD14+ cells cultured in M-CSF alone compared to M-CSF and RANKL in combination. Using TRITC-conjugated phalloidin, we labeled the F-actin cytoskeleton in cells grown on bone slices. RANKL

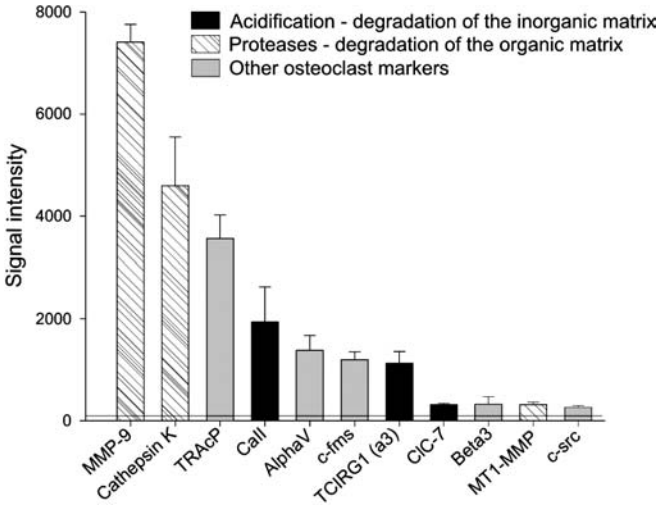

Fig. 4. Affymetrix analysis of osteoclast markers. Mature human osteoclasts were seeded on giant-sized bone slices, and after 2 days of attachment and initiation of resorption the RNA was extracted and the mRNA was isolated and hybridized to the affymetrix array. The results are shown as average expression of the detected number of probes; the *horizontal line* indicates the average expression of all detected probes on the array

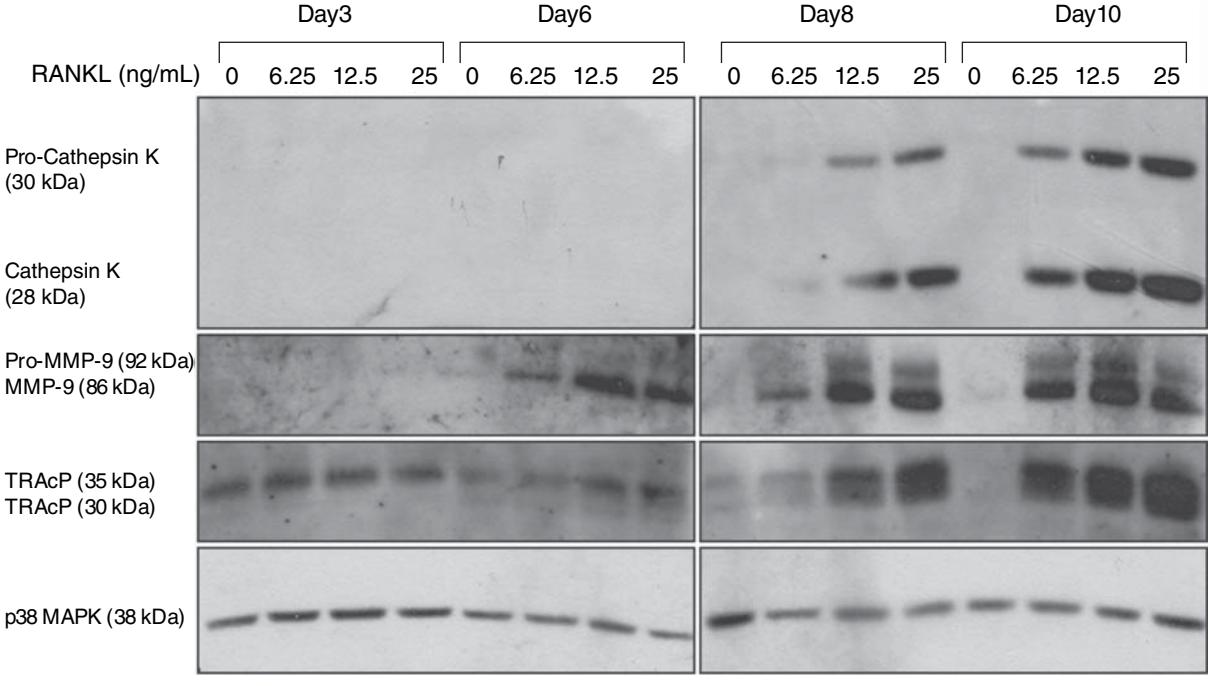

Fig. 5. Increasing concentrations of RANKL leads to an increase expression of osteoclast markers. CD14+ monocytes were seeded in 6-well plates, cultured in the presence of M-CSF (25 ng/ml) and 0, 6.25, 12.5, or 25 ng/ml RANKL for 3, 6, 8, or 10 days, and then lysed as described in the Materials and methods section. The expression of osteoclast markers was analyzed by loading the lysates on SDS-PAGE gels with subsequent immunoblotting

treatment leads to the formation of the osteoclastic resorption lacunae, as visualized by the formation of the actin rings (Fig. 6A). In contrast, in the M-CSF condition alone, only cells with macrophage morphology were observed [48–50].

We then characterized the expression and localization of the calcitonin receptor, cathepsin K, ClC-7, MMP-9, TRACP, and c-*src* by comparing the cells treated in the presence or absence of RANKL. The calcitonin receptor was localized mainly on the cell surface, whereas cathepsin K, ClC-7, MMP-9, TRACP, and c-*src* all were localized in gradients toward the resorption lacunae (Fig. 6B). In the M-CSF condition, no expression of cathepsin K, MMP-9 and c-*src* was seen, whereas a low and intracellular staining of ClC-7, TRACP, and the calcitonin receptor was seen. However, the staining was stronger in the M-CSF- and RANKL-treated cells.

Acidification of the osteoclast resorption lacunae

Ability to acidify the resorption lacuna is essential for osteoclast function [51]. We used the dye acridine orange, which emits a bright orange fluorescence at pH between 4 and 5, as observed in the resorption lacunae [52], to investigate the response of the human osteoclasts to known resorption inhibitors. Osteoclasts in the absence of inhibitors exhibit a bright orange fluorescence, indicating the formation of a resorption lacuna (Fig. 7). Addition of the V-ATPase inhibitor, bafilomycin A1, and ClC-7 inhibitor, NS5818, led to complete abrogation of the orange signal, showing that these compounds as expected inhibit acidification of the resorption lacunae [53,54]. Furthermore, addition of E64, a cysteine proteinase inhibitor, which mainly inhibits cathepsin K activity from the osteoclasts, had no effect on the acidification process. Addition of ethoxyzolamide, which inhibits carbonic anhydrase II, had no effect on the acidification. Carbonic anhydrase II catalyzes the process, which provides protons to the V-ATPase, and hereby ethoxyzolamide will inhibit bone resorption with time. However, the process to form bicarbonate and protons from carbon dioxide and water is an exergonic process, and the production of bicarbonate and protons will continue for a time, even though the process is not catalyzed by carbonic anhydrase II.

Inhibitors of resorption

In vitro generated osteoclasts are often used to study biological processes, such as signal transduction, or for investigating the antiresorptive properties of compounds in clinical development programs of osteoporosis treatment.

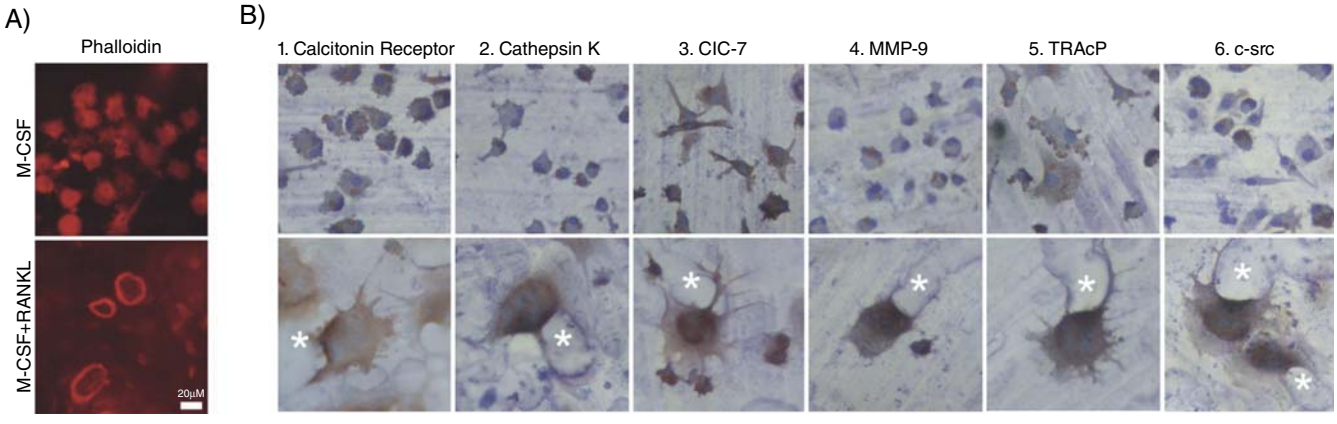

Fig. 6. Cells with osteoclast morphology are only seen in the presence of RANKL. CD14+ monocytes were isolated and cultured on cortical bone slices in the presence of M-CSF alone or in combination with RANKL for 18 days. **A** Visualization of the actin cytoskeleton in the absence or presence of RANKL. **B** Immunolocalization of (*1*) calcitonin receptor; (*2*) cathepsin K; (*3*) ClC-7; (*4*) matrix metallo proteinase (MMP)-9; (*5*) TRACP; and (*6*) c-*src*. Asterisks (B) indicate the resorption lacunae. (20× magnification (A,B))

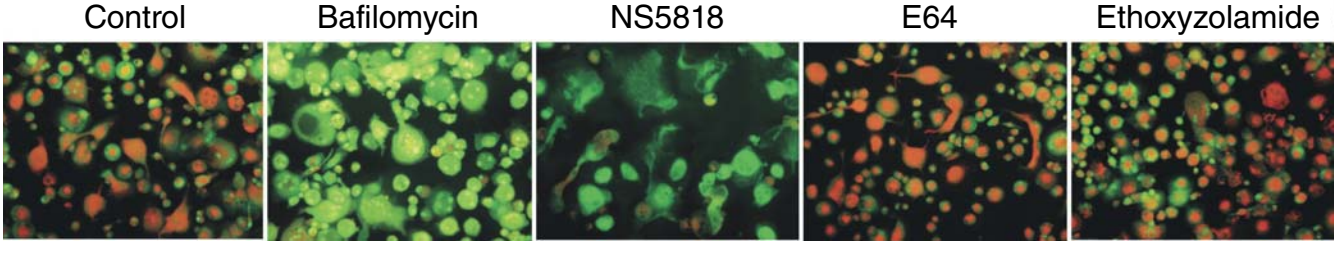

Fig. 7. Acidification of the resorption lacunae visualized using acridine orange. Mature human osteoclasts were seeded on glass coverslips and allowed to attach for 2 days. The cells were then incubated for 45 min with acridine orange alone or in combination with the following inhibitors: bafilomycin A1, NS5818, E64, and ethoxyzolamide (20× magnification)

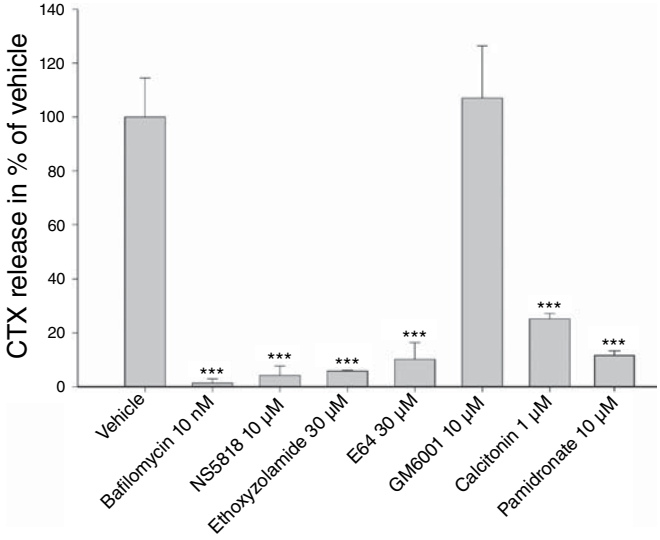

Fig. 8. The osteoclast assay is stable and sensitive to known inhibitors of resorption. Mature human osteoclasts were seeded on cortical bovine bone slices and allowed to attach. After 2 days of culture, the different inhibitors were added to the culture for another 2 days. CTX-I release was measured in the culture supernatant, the results are presented as relative inhibition compared to vehicle-treated osteoclasts. The following inhibitors were used: bafilomycin A1, NS5818, ethoxyzolamide, E64, GM6001, calcitonin, and pamidronate. The *asterisks* indicate significant differences between the control condition and the inhibitor-treated conditions

We tested several compounds known to inhibit resorption in different osteoclast systems; these include inhibitors of the V-ATPase (bafilomycin A1), the chloride channel ClC-7 (NS5818), cathepsin K (E64), MMPs (GM6001), carbonic anhydrase II (ethoxyzolamide), as well as calcitonin and the bisphosphonate pamidronate. All the inhibitors except GM6001 inhibited osteoclast resorption efficiently (Fig. 8) [54–58]. GM6001 has previously been shown to inhibit resorption on bones derived from calvariae or other flat bones [59], whereas it does not inhibit resorption on cortical bones [45,60]. Thus, the osteoclast resorption system here accurately and robustly allows for screening of antiresorptive compounds.

Discussion

Studies of human osteoclasts were, until the discovery of RANKL and the finding that the osteoclast precursors reside in the CD14+ monocyte fraction, difficult and unclear because of contaminating cells of both stromal and lymphocyte origin [41,42]. We have developed a pure, robust, and reproducible human osteoclast system based on isolation of CD14+ monocytes using magnetic bead sorting. In this article, we have provided a detailed description of the method and several very useful assays for characterization of osteoclast differentiation and function.

First, we showed that the system is pure, as we only observed osteoclast formation and activity in the presence of RANKL, which indicates that neither stromal cells nor lymphocytes, which both have the ability to induce osteoclast formation, were present [61–64]. Second, we showed that CD14– cells do not possess the ability to differentiate into osteoclasts, as most of them are nonadherent and therefore lost during culture, in line with a previous publication showing that removal of nonadherent cells augments the osteoclastogenic potential of nonsorted peripheral blood mononuclear cells [48]. We then showed that human osteoclasts differentiated from CD14+ monocytes express mRNA for several osteoclast markers. Furthermore, we analyzed the expression of the osteoclastic markers cathepsin K, MMP-9, and TRACP in response to different concentrations of RANKL. We found that these markers were dose-dependently induced by the RANKL treatment with different onsets of expression. At day 8 and at 12.5–25 ng/ml RANKL, the purified monocytes have differentiated into mature osteoclasts expressing cathepsin K, MMP-9, and TRACP. The lack of cathepsin K expression before day 8 correlates with cathepsin K as a marker for bone resorption; this is in correlation with the CTX-I release, which is initiated at day 9 for differentiating osteoclasts (see Fig. 2). In contrast to this, TRACP expression was seen before cathepsin K expression, already at day 3, and before bone resorption, indicating that TRACP is not a marker for resorption but an indication of osteoclast number.

We showed that only in the presence of RANKL do the cells differentiate into actin ring-forming osteoclasts. By immunocytochemistry, we investigated the localization of osteoclast markers, comparing the RANKL-treated cells with the non-RANKL-treated. As expected, ClC-7, c-*src*, MMP-9, TRACP, and cathepsin K localized in gradients toward the resorption lacuna in the osteoclasts [60,65], whereas we observed no expression of cathepsin K, MMP-9, and c-*src* in the non-RANKL-treated cells. However, we observed low and intracellular ClC-7, calcitonin receptor, and TRACP expression in these cells. To a lesser extent, expression of ClC-7, TRACP, and the calcitonin receptor was found in the cells treated only with M-CSF; this may be as a consequence of signals from the bone surface to the preosteoclasts, in addition to the well-known essential factors M-CSF and RANKL. This finding is supported by the fact that monocytes grown in the presence of M-CSF alone on plastic did not display TRACP activity, as measured by Western blotting (see Fig. 5). Thus, the signals for monocytes to become real osteoclasts may both depend on M-CSF and RANKL, and in addition depend on factors on the bone surface that interact with special integrins in osteoclasts, recognizing in particular collagen type 1 [65,66]. This finding correlates with the observation that mature osteoclasts only are found on bone [44].

We have described a robust system for purification of human monocytes and differentiation of these into mature osteoclasts, which can be used to study the mode of action in osteoclasts. In the current studies, we employed this feature to further investigate the mode of action of resorption inhibition in osteoclasts, by investigation of acidification of the osteoclastic resorption lacunae, by acridine orange. Thus, the current system is a powerful technique to further

investigate the mode of action of new compounds that potentially could be interfering with osteoclast function, and thereby be potential drugs for the treatment of bone-related diseases.

In conclusion, we have developed a stable system for the specific differentiation of human osteoclasts that can be used to study the function of mature human osteoclasts, their differentiation, and the mode of action of various compounds. The current study presented detailed data on osteoclast generation that may aid other researchers in studies of osteoclastogenesis.

References

1. Baron R (2003) General principles of bone biology. In: The American Society for Bone and Mineral Research (eds) Primer on the Metabolic Bone Diseases and Disorders of Mineral Metabolism. Lippincott-Raven, New York, pp 1–9
2. Marks SC, Hermey DC (1996) The structure and development of bone. In: Bilezikian JP, Raisz LG, Rodan GA (eds) Principles of Bone Biology. Academic Press, San Diego, pp 3–14
3. Vaananen HK (1993) Mechanism of bone turnover. Ann Med 25:353–359
4. Mundy GR (1996) Bone-resorbing cells. In: The American Society for Bone and Mineral Research (ed) Primer on the Metabolic Bone Diseases and Disorders of Mineral Metabolism. Lippincott-Raven, New York, pp 16–24
5. Suda T, Udagawa N, Takahashi N (1996) Cells of bone: osteoclast generation. In: Bilezikian JP, Raisz LG, Rodan GA (eds) Principles of Bone Biology. Academic press, San Diego, pp 87–102
6. Baron R, Neff L, Tran VP, Nefussi JR, Vignery A (1986) Kinetic and cytochemical identification of osteoclast precursors and their differentiation into multinucleated osteoclasts. Am J Pathol 122:363–378
7. Ibbotson KJ, Roodman GD, McManus LM, Mundy GR (1984) Identification and characterization of osteoclast-like cells and their progenitors in cultures of feline marrow mononuclear cells. J Cell Biol 99:471–480
8. Osdoby P, Martini MC, Caplan AI (1982) Isolated osteoclasts and their presumed progenitor cells, the monocyte, in culture. J Exp Zool 224:331–344
9. Lacey DL, Timms E, Tan HL, Kelley MJ, Dunstan CR, Burgess T, Elliott R, Colombero A, Elliott G, Scully S, Hsu H, Sullivan J, Hawkins N, Davy E, Capparelli C, Eli A, Qian YX, Kaufman S, Sarosi I, Shalhoub V, Senaldi G, Guo J, Delaney J, Boyle WJ (1998) Osteoprotegerin ligand is a cytokine that regulates osteoclast differentiation and activation. Cell 93:165–176
10. Roodman GD (1999) Cell biology of the osteoclast. Exp Hematol 27:1229–1241
11. Teitelbaum SL (2000) Bone resorption by osteoclasts. Science 289:1504–1508
12. Lakkakorpi PT, Vaananen HK (1996) Cytoskeletal changes in osteoclasts during the resorption cycle. Microsc Res Tech 33:171–181
13. Vaananen HK, Horton M (1995) The osteoclast clear zone is a specialized cell-extracellular matrix adhesion structure. J Cell Sci 108(pt 8):2729–2732
14. Lakkakorpi P, Tuukkanen J, Hentunen T, Jarvelin K, Vaananen K (1989) Organization of osteoclast microfilaments during the attachment to bone surface in vitro. J Bone Miner Res 4:817–825
15. Väänänen K (1996) Osteoclast function: biology and mechanisms. In: Bilezikian JP, Raisz LG, Rodan GA (eds) Principles of Bone Biology. Academic Press, San Diego, pp 103–113
16. Baron R, Neff L, Louvard D, Courtoy PJ (1985) Cell-mediated extracellular acidification and bone resorption: evidence for a low pH in resorbing lacunae and localization of a 100-kD lysosomal membrane protein at the osteoclast ruffled border. J Cell Biol 101:2210–2222
17. Li YP, Chen W, Liang Y, Li E, Stashenko P (1999) Atp6i-deficient mice exhibit severe osteopetrosis due to loss of osteoclast-mediated extracellular acidification. Nat Genet 23:447–451
18. Taranta A, Migliaccio S, Recchia I, Caniglia M, Luciani M, De Rossi G, Dionisi-Vici C, Pinto RM, Francalanci P, Boldrini R, Lanino E, Dini G, Morreale G, Ralston SH, Villa A, Vezzoni P, Del Principe D, Cassiani F, Palumbo G, Teti A (2003) Genotype-phenotype relationship in human ATP6i-dependent autosomal recessive osteopetrosis. Am J Pathol 162:57–68
19. Sundquist K, Lakkakorpi P, Wallmark B, Vaananen K (1990) Inhibition of osteoclast proton transport by bafilomycin A1 abolishes bone resorption. Biochem Biophys Res Commun 168:309–313
20. al Awqati Q (1995) Chloride channels of intracellular organelles. Curr Opin Cell Biol 7:504–508
21. Schlesinger PH, Blair HC, Teitelbaum SL, Edwards JC (1997) Characterization of the osteoclast ruffled border chloride channel and its role in bone resorption. J Biol Chem 272:18636–18643
22. Toyomura T, Oka T, Yamaguchi C, Wada Y, Futai M (2000) Three subunit a isoforms of mouse vacuolar H(+)-ATPase. Preferential expression of the a3 isoform during osteoclast differentiation. J Biol Chem 275:8760–8765
23. Manolson MF, Yu H, Chen W, Yao Y, Li K, Lees RL, Heersche JN (2003) The a3 isoform of the 100-kDa V-ATPase subunit is highly but differentially expressed in large (> or = 10 nuclei) and small (< or = nuclei) osteoclasts. J Biol Chem 278:49271–49278
24. Kornak U, Schulz A, Friedrich W, Uhlhaas S, Kremens B, Voit T, Hasan C, Bode U, Jentsch TJ, Kubisch C (2000) Mutations in the a_3 subunit of the vacuolar H(+)-ATPase cause infantile malignant osteopetrosis. Hum Mol Genet 9:2059–2063
25. Kornak U, Kasper D, Bosl MR, Kaiser E, Schweizer M, Schulz A, Friedrich W, Delling G, Jentsch TJ (2001) Loss of the ClC-7 chloride channel leads to osteopetrosis in mice and man. Cell 104:205–215
26. Vaananen HK, Zhao H, Mulari M, Halleen JM (2000) The cell biology of osteoclast function. J Cell Sci 113(pt 3):377–381
27. Gowen M, Lazner F, Dodds R, Kapadia R, Feild J, Tavaria M, Bertoncello I, Drake F, Zavarselk S, Tellis I, Hertzog P, Debouck C, Kola I (1999) Cathepsin K knockout mice develop osteopetrosis due to a deficit in matrix degradation but not demineralization. J Bone Miner Res 14:1654–1663
28. Littlewood-Evans A, Kokubo T, Ishibashi O, Inaoka T, Wlodarski B, Gallagher JA, Bilbe G (1997) Localization of cathepsin K in human osteoclasts by in situ hybridization and immunohistochemistry. Bone (NY) 20:81–86
29. Nishi Y, Atley L, Eyre DE, Edelson JG, Superti-Furga A, Yasuda T, Desnick RJ, Gelb BD (1999) Determination of bone markers in pycnodysostosis: effects of cathepsin K deficiency on bone matrix degradation. J Bone Miner Res 14:1902–1908
30. Saftig P, Hunziker E, Wehmeyer O, Jones S, Boyde A, Rommerskirch W, Moritz JD, Schu P, von Figura K (1998) Impaired osteoclastic bone resorption leads to osteopetrosis in cathepsin-K-deficient mice. Proc Natl Acad Sci U S A 95:13453–13458
31. Stroup GB, Lark MW, Veber DF, Bhattacharyya A, Blake S, Dare LC, Erhard KF, Hoffman SJ, James IE, Marquis RW, Ru Y, Vasko-Moser JA, Smith BR, Tomaszek T, Gowen M (2001) Potent and selective inhibition of human cathepsin K leads to inhibition of bone resorption in vivo in a nonhuman primate. J Bone Miner Res 16:1739–1746
32. Everts V, Aronson DC, Beertsen W (1985) Phagocytosis of bone collagen by osteoclasts in two cases of pycnodysostosis. Calcif Tissue Int 37:25–31
33. Motyckova G, Fisher DE (2002) Pycnodysostosis: role and regulation of cathepsin K in osteoclast function and human disease. Curr Mol Med 2:407–421
34. Garnero P, Borel O, Byrjalsen I, Ferreras M, Drake FH, McQueney MS, Foged NT, Delmas PD, Delaisse JM (1998) The collagenolytic activity of cathepsin K is unique among mammalian proteinases. J Biol Chem 273:32347–32352
35. Boyle WJ, Simonet WS, Lacey DL (2003) Osteoclast differentiation and activation. Nature (Lond) 423:337–342
36. Manolagas SC (2000) Birth and death of bone cells: basic regulatory mechanisms and implications for the pathogenesis and treatment of osteoporosis. Endocr Rev 21:115–137

37. Nicholson GC, Moseley JM, Sexton PM, Mendelsohn FA, Martin TJ (1986) Abundant calcitonin receptors in isolated rat osteoclasts. Biochemical and autoradiographic characterization. J Clin Invest 78:355–360
38. Horton M (1990) Vitronectin receptor: tissue specific expression or adaptation to culture? Int J Exp Pathol 71:741–759
39. Davies J, Warwick J, Totty N, Philp R, Helfrich M, Horton M (1989) The osteoclast functional antigen, implicated in the regulation of bone resorption, is biochemically related to the vitronectin receptor. J Cell Biol 109:1817–1826
40. Okada Y, Naka K, Kawamura K, Matsumoto T, Nakanishi I, Fujimoto N, Sato H, Seiki M (1995) Localization of matrix metalloproteinase 9 (92-kilodalton gelatinase/type IV collagenase = gelatinase B) in osteoclasts: implications for bone resorption. Lab Invest 72:311–322
41. Massey HM, Flanagan AM (1999) Human osteoclasts derive from CD14-positive monocytes. Br J Haematol 106:167–170
42. Nicholson GC, Malakellis M, Collier FM, Cameron PU, Holloway WR, Gough TJ, Gregorio-King C, Kirkland MA, Myers DE (2000) Induction of osteoclasts from CD14-positive human peripheral blood mononuclear cells by receptor activator of nuclear factor kappaB ligand (RANKL). Clin Sci (Lond) 99:133–140
43. Li C, Wong W (2003) DNA-chip analyser (dChip). In: Parmigiani G, Garret ES, Irizarry R, Zeger SL (eds) The Analysis of Gene Expression Data: Methods and Software. Springer, New York, pp 120–141
44. Engsig MT, Chen QJ, Vu TH, Pedersen AC, Therkidsen B, Lund LR, Henriksen K, Lenhard T, Foged NT, Werb Z, Delaisse JM (2000) Matrix metalloproteinase 9 and vascular endothelial growth factor are essential for osteoclast recruitment into developing long bones. J Cell Biol 151:879–889
45. Henriksen K, Gram J, Schaller S, Dahl BH, Dziegiel MH, Bollerslev J, Karsdal MA (2004) Characterization of osteoclasts from patients harboring a G215R mutation in ClC-7 causing autosomal dominant osteopetrosis type II. Am J Pathol 164:1537–1545
46. Schaller S, Henriksen K, Sveigaard C, Heegaard A, Hélix N, Stahlhut M, Ovejero MC, Johansen JV, Solberg H, Andersen TL, Hougaard D, Shiøt CB, Sørensen BH, Lichtenberg J, Christophersen P, Foged NT, Delaissé J, Engsig MT, Karsdal MA (2004) The chloride channel inhibitor NS3736 prevents bone resorption in ovariectomized rats without changing bone formation. J Bone Miner Res 19:1144–1153
47. Henriksen K, Karsdal M, Delaisse JM, Engsig MT (2003) RANKL and vascular endothelial growth factor (VEGF) induce osteoclast chemotaxis through an ERK1/2-dependent mechanism. J Biol Chem 278:48745–48753
48. Karsdal MA, Hjorth P, Henriksen K, Kirkegaard T, Nielsen KL, Lou H, Delaisse JM, Foged NT (2003) Transforming growth factor-beta controls human osteoclastogenesis through the p38 MAPK and regulation of RANK expression. J Biol Chem 278:44975–44987
49. Quinn JM, Neale S, Fujikawa Y, McGee JO, Athanasou NA (1998) Human osteoclast formation from blood monocytes, peritoneal macrophages, and bone marrow cells. Calcif Tissue Int 62:527–531
50. Shalhoub V, Elliott G, Chiu L, Manoukian R, Kelley M, Hawkins N, Davy E, Shimamoto G, Beck J, Kaufman SA, Van G, Scully S, Qi M, Grisanti M, Dunstan C, Boyle WJ, Lacey DL (2000) Characterization of osteoclast precursors in human blood. Br J Haematol 111:501–512
51. Blair HC, Teitelbaum SL, Ghiselli R, Gluck S (1989) Osteoclastic bone resorption by a polarized vacuolar proton pump. Science 245:855–857
52. Silver IA, Murrills RJ, Etherington DJ (1988) Microelectrode studies on the acid microenvironment beneath adherent macrophages and osteoclasts. Exp Cell Res 175:266–276
53. Yoshimori T, Yamamoto A, Moriyama Y, Futai M, Tashiro Y (1991) Bafilomycin A1, a specific inhibitor of vacuolar-type H(+)-ATPase, inhibits acidification and protein degradation in lysosomes of cultured cells. J Biol Chem 266:17707–17712
54. Karsdal MA, Henriksen K, Sorensen MG, Gram J, Schaller S, Dziegiel MH, Heegaard AM, Christophersen P, Martin TJ, Christiansen C, Bollerslev J (2005) Acidification of the osteoclastic resorption compartment provides insight into the coupling of bone formation to bone resorption. Am J Pathol 166:467–476
55. Bowman EJ, Siebers A, Altendorf K (1988) Bafilomycins: a class of inhibitors of membrane ATPases from microorganisms, animal cells, and plant cells. Proc Natl Acad Sci U S A 85:7972–7976
56. Falgueyret JP, Oballa RM, Okamoto O, Wesolowski G, Aubin Y, Rydzewski RM, Prasit P, Riendeau D, Rodan SB, Percival MD (2001) Novel, nonpeptidic cyanamides as potent and reversible inhibitors of human cathepsins K and L. J Med Chem 44:94–104
57. Hall TJ, Higgins W, Tardif C, Chambers TJ (1991) A comparison of the effects of inhibitors of carbonic anhydrase on osteoclastic bone resorption and purified carbonic anhydrase isozyme II. Calcif Tissue Int 49:328–332
58. Kellinsalmi M, Monkkonen H, Monkkonen J, Leskela HV, Parikka V, Hamalainen M, Lehenkari P (2005) In vitro comparison of clodronate, pamidronate and zoledronic acid effects on rat osteoclasts and human stem cell-derived osteoblasts. Basic Clin Pharmacol Toxicol 97:382–391
59. Garnero P, Ferreras M, Karsdal MA, Nicamhlaoibh R, Risteli J, Borel O, Qvist P, Delmas PD, Foged NT, Delaisse JM (2003) The type I collagen fragments ICTP and CTX-I reveal distinct enzymatic pathways of bone collagen degradation. J Bone Miner Res 18:859–867
60. Henriksen K, Sorensen MG, Nielsen RH, Gram J, Schaller S, Dziegiel MH, Everts V, Bollerslev J, Karsdal MA (2006) Degradation of the organic phase of bone by osteoclasts: a secondary role for lysosomal acidification. J Bone Miner Res 21:58–66
61. Udagawa N, Takahashi N, Akatsu T, Tanaka H, Sasaki T, Nishihara T, Koga T, Martin TJ, Suda T (1990) Origin of osteoclasts: mature monocytes and macrophages are capable of differentiating into osteoclasts under a suitable microenvironment prepared by bone marrow-derived stromal cells. Proc Natl Acad Sci U S A 87:7260–7264
62. Kotake S, Udagawa N, Hakoda M, Mogi M, Yano K, Tsuda E, Takahashi K, Furuya T, Ishiyama S, Kim KJ, Saito S, Nishikawa T, Takahashi N, Togari A, Tomatsu T, Suda T, Kamatani N (2001) Activated human T cells directly induce osteoclastogenesis from human monocytes: possible role of T cells in bone destruction in rheumatoid arthritis patients. Arthritis Rheum 44:1003–1012
63. Weitzmann MN, Cenci S, Rifas L, Haug J, Dipersio J, Pacifici R (2001) T cell activation induces human osteoclast formation via receptor activator of nuclear factor kappaB ligand-dependent and -independent mechanisms. J Bone Miner Res 16:328–337
64. Horwood NJ, Kartsogiannis V, Quinn JM, Romas E, Martin TJ, Gillespie MT (1999) Activated T lymphocytes support osteoclast formation in vitro. Biochem Biophys Res Commun 265:144–150
65. Teitelbaum SL, Ross FP (2003) Genetic regulation of osteoclast development and function. Nat Rev Genet 4:638–649
66. Meredith JE Jr, Winitz S, Lewis JM, Hess S, Ren XD, Renshaw MW, Schwartz MA (1996) The regulation of growth and intracellular signaling by integrins. Endocr Rev 17:207–220